Published in final edited form as:
Chem Res Toxicol. 2010 May 17; 23(5): 933–938. doi:10.1021/tx100022x.

Oxidation of 8-Oxo-7,8-dihydro-2′-deoxyguanosine by Oxyl Radicals Produced by Photolysis of Azo Compounds

Jie Shao, **Nicholas E. Geacintov**, and **Vladimir Shafirovich***
Chemistry Department, 31 Washington Place, New York University, New York, New York 10003-5180

Abstract

Oxidative damage to 8-oxo-7,8-dihydroguanine (8-oxoG) bases initiated by photolysis of the water-soluble radical generator 2,2′-azobis(2-amidinopropane) dihydrochloride (AAPH) has been investigated by laser kinetic spectroscopy. In neutral oxygenated aqueous solutions, 355 nm photolysis of AAPH initiates efficient one-electron oxidation of the 8-oxodG nucleosides directly monitored by the appearance of the 8-oxodG$^{\bullet+}$/8-oxodG(-H)$^{\bullet}$ radicals at 325 nm. The reaction kinetics are consisted with a mechanism that includes the transformation of the 2-amidinoprop-2-peroxyl radicals (ROO$^{\bullet}$) derived from photolysis of AAPH to more reactive 2-amidinoprop-2-oxyl radicals (RO$^{\bullet}$), which directly react with the 8-oxoG bases. The major pathways for the formation of end products of 8-oxoG oxidation include the combination of the 8-oxodG$^{\bullet+}$/8-oxodG(-H)$^{\bullet}$ radicals with superoxide ($O_2^{\bullet-}$) and ROO$^{\bullet}$ radicals in approximately 1:1 ratios, as demonstrated by experiments with Cu, Zn superoxide dismutase to form dehydroguanidinohydantoin (Gh_{ox}) derivatives. This mechanism was confirmed by analysis of the end products produced by the oxidation of two substrates: (1) the 8-oxoG derivative 2′,3′,5′-tri-*O*-acetylguanosine (tri-*O*-Ac-G), and (2) the 5′-d(CCATC[8-oxoG]CTACC) sequence. The major products isolated by HPLC and identified by mass spectrometry methods were the tri-*O*-Ac-Gh_{ox} and 5′-d(CCATC[Gh_{ox}]CTACC products.

Introduction

Persistent oxidative damage to cellular DNA associated with chronic inflammation developed in response to microbial and viral infections, tobacco smoke, and other environmental insults, is genotoxic and has been implicated in the etiology of many human cancers (1). The most common DNA lesion detected in vivo is 8-oxo-7,8-dihydroguanine (8-oxoG),[1] a well-known biomarker of oxidative stress (2). This lesion is mutagenic because it mispairs with A during replication by DNA polymerases that lead to a predominant G → T transversion mutation (3), the second most common somatic mutation in human carcinomas (4). The oxidation products of 8-oxoG, which is more easily oxidizable than any of the natural nucleic acid bases (5), are more mutagenic than the parent 8-oxoG (6–8). Lipid peroxyl radicals are ubiquitous free radicals in biological systems (reviewed in (9,10)) that, potentially, can selectively oxidize 8-oxoG residues in vivo (11). However, the mechanisms of reaction of these radicals with 8-oxoG remain poorly understood because of complexities associated with the interconversion

*To whom the correspondence should be addressed. Chemistry Department, 31 Washington Place, New York University, New York, New York 10003-5181. Tel.: (212) 998 8456; Fax: (212) 998 8421; vs5@nyu.edu.

[1]The abbreviations used are: 8-oxoG, 8-oxo-7,8-dihydroguanine; 8-oxodG, 8-oxo-7,8-dihydro-2′-deoxyguanosine; dR, 2-deoxy-*β*-D-ribofuranosyl; AAPH, 2,2′-azobis(2-amidinopropane) dihydrochloride; ROO$^{\bullet}$, 2-amidinoprop-2-peroxyl; RO$^{\bullet}$, 2-amidinoprop-2-oxyl radical; R$^{\bullet}$, 2-amidinopropyl radical; tri-*O*-ac-8-oxoGuo, 2′,3′,5′-tri-*O*-acetyl-8-oxo-7,8-dihydroguanosine; ArAc, arachidonic acid; PcAc, 3-pentenoic acid; Gh_{ox}, dehydroguanidinohydantoin; Sp, spiroiminodihydantoin; $O_2^{\bullet-}$, superoxide radical anion.

and fragmentation of lipid peroxyl and alkoxyl radicals that have not been structurally characterized.

The thermal and photochemical decomposition of azo compounds is a classical approach for the controlled generation of alkylperoxyl radicals (12). The water-soluble 2,2′-azobis(2-amidinopropane) dihydrochloride (known as ABAP (13) or AAPH (14)) has been extensively used to initiate lipid peroxidation (15–17), in order to explore the effects of oxidative stress on cultured cells (18–21), oxidation of DNA (22–24), and signaling responses associated with inflammation and aging (25). Our own laser flash photolysis experiments have shown that the photolysis of AAPH generates a whole spectrum of free radicals including 2-amidinoprop-2-peroxyl ($ROO^{\bullet}$), 2-amidinoprop-2-oxyl ($RO^{\bullet}$), and superoxide ($O_2^{\bullet-}$) radicals (26). We found that $RO^{\bullet}$ radicals induce the fast one-electron oxidation of 2′-deoxyguanosine (dG) to form guanine neutral radicals, $dG(-H)^{\bullet}$. In contrast, $ROO^{\bullet}$ radicals do not react with observable rates with dG. The major pathway for the formation of the end products of guanine oxidation is the combination of the $G(-H)^{\bullet}$ and $O_2^{\bullet-}$ radicals to form 2,5-diamino-4*H*-imidazolone (Iz) (26).

In this work we investigated the kinetics of 8-oxoguanine oxidation by free radicals generated by the photolysis of AAPH in neutral aqueous solutions. These kinetic laser flash photolysis experiments show that 2-amidinoprop-2-oxyl radicals derived from the combination of 2-amidinoprop-2-peroxyl radicals induce the rapid one-electron oxidation of 8-oxodG (Figure 1).

It is shown that the major pathway for the formation of the end products of 8-oxoG oxidation in either 2′,3′,5′-tri-*O*-acetyl-8-oxo-7,8-dihydroguanosine (tri-*O*-Ac-8-oxoG) or the 5′-d(CCATC[8-oxoG]CTACC) oligonucleotoide sequence, is the combination of $8\text{-oxoG}(-H)^{\bullet}$ and $O_2^{\bullet-}$ radicals to form dehydroguanidinohydantoin (Gh_{ox}).

Experimental Procedures

Materials

Analytical grade chemicals, HPLC grade organic solvents, and Milli-Q purified (ASTM type I) water were used throughout; 2,2′-azobis(2-amidinopropane) dihydrochloride and 2′,3′,5′-tri-*O*-acetyl-8-bromoguanosine from Sigma-Aldrich (St. Louis, MO), and 8-oxo-7,8-dihydro-2′-deoxyguanosine from Berry and Associates, Inc. (Dexter, MI) were used as received. The 2′,3′,5′-tri-*O*-acetyl-8-oxo-7,8-dihydroguanosine was synthesized by hydrolysis of tri-*O*-acetyl-8-bromoguanosine as described previously (27). The 5′-d(GGATC[8-oxoG]CTACC) sequence from Biosynthesis Inc. (Lewisville, TX) was purified, and desalted using reversed-phase HPLC. The integrity of the nucleosides and oligonucleotides was confirmed by the LC-MS/MS and MALDI-TOF/MS analysis. Phosphate buffer solutions were tested for residual traces of transition metals and, if necessary, were treated with Chelex (28).

Laser Flash Photolysis

The transient absorption spectra and kinetics of free radical reactions were monitored directly using a fully-computerized kinetic spectrometer system (~7 ns response time) described elsewhere (29). In this work, a 355 nm Nd: Yag laser (Continuum NY 81-20) was used to photolyse the samples in a quartz micro flow cell (~ 100 μL). The single laser pulses were selected from the nanosecond pulse trains (4–20 mJ/cm^2/pulse, 20 Hz) by a computer-controlled electromechanical shutter. To avoid the effects of photoinduced decomposition of the samples, fresh solutions were injected into irradiated volume by mixing, two solutions (e.g., AAPH and 8-oxodG) by forcing each into a mixer by a small positive gas pressure (0.3–0.5 atm) and then through the cell at a flow rate of 6–8 mL/min; the laser excitation occurred within less than 1 s after mixing. The solution flow was controlled by two solenoid valves to provide

a complete sample replacement between successive laser shots. The transient absorbance was probed along a 1 cm optical path by light from a pulsed 75 W xenon arc lamp with its light beam oriented perpendicular to the laser beam. The signal was recorded by a Tektronix TDS 5052 oscilloscope operating in its high-resolution mode that typically allows for a suitable signal/noise ratio after a single laser short. All experiments were performed at room temperature (23±2 °C). The rate constants of the free radical reactions were typically determined by least squares fits of the appropriate kinetic equations to the transient absorption profiles obtained in five different experiments with five different samples.

Photochemical Oxidation of 8-Oxoguanine

The samples of 100 nmol tri-*O*-acetyl-8-oxoG, or 10 nmol 5′-d(GGATC[8-oxoG]CTACC) in 1 mL air-equilibrated 5 mM phosphate buffer solutions, pH 7.0 containing 20 mM AAPH were irradiated for fixed periods by a light beam of a 100 W xenon arc lamp reflected at 45° from a dielectric mirror to select the 340–390 nm spectral range for photolysis. The irradiated samples were immediately subjected to analysis by HPLC methods. The chemical structures of the Gh_{ox} and nucleosides were confirmed by LC-MS/MS analysis of the isolated end products and by comparisons with authentic standards.

Mass spectrometry assays

LC-MS analysis of the photoproducts was performed with an Agilent 1100 Series capillary LC/MSD Ion Trap XCT mass spectrometer equipped with an electrospray ion source as described elsewhere.(30) The MALDI-TOF mass spectra were recorded in the negative mode using a Bruker OmniFLEX instrument.

Results and Discussion

One-Electron Oxidation of 8-OxodG Initiated by Photolysis of AAPH

Photolysis of AAPH by 355 nm laser pulses in air-equilibrated neutral buffer solutions (pH 7.0) induces efficient one-electron oxidation of 8-oxo-7,8-dihydro-2′-deoxyguanosine. The 8-oxodG radicals, which are the products of this reaction, were identified by the appearance of the characteristic narrow absorption band at 325 nm (11,31,32) as shown in Figure 2.

The presence of AAPH is critical for the oxidation of 8-oxo-dG. The 8-oxodG does not absorb at 355 nm and in typical experiments the laser flash photolysis of the 8-oxodG solutions (no AAPH) using this excitation wavelength does not produce a detectable signal at 325 nm. In turn, increasing the concentration of AAPH from 5 to 30 mM, or the laser pulse energy in the range of 4–20 mJ/pulse/cm^2 in the latter case, induces an approximately linear increase in the transient absorbance at 325 nm (data not shown). Furthermore, the presence of oxygen is also required for the oxidation 8-oxo-dG. Indeed, only small changes in the transient absorbance are observed in argon-purged solutions (blue line, insert in Figure 2).

At pH 7 the 8-oxodG$^{\bullet+}$ radical cation (pK_a = 6.6) produced by a one-electron abstraction from 8-oxodG is in equilibrium with its neutral form, 8-oxodG(-H)$^{\bullet}$, and the absorption band at 325 nm (Figure 2) can be assigned to the mixture of the cation and neutral forms, which have very similar absorption spectra (11). The kinetic profiles recorded at 325 nm and associated with the growth of the 8-oxodG$^{\bullet+}$/8-oxodG(-H)$^{\bullet}$ absorbance exhibit a characteristic S-like shape (inset in Figure 2). The formation of 8-oxodG$^{\bullet+}$/8-oxodG(-H)$^{\bullet}$ becomes efficient after the initial 10–15 μs and is complete 120–150 μs after the actinic laser flash. The yields of the 8-oxodG$^{\bullet+}$/8-oxodG(-H)$^{\bullet}$ radicals (Y_{8oGR}) calculated at Δt = 120–150 μs using the extinction coefficient (11), $\varepsilon_{325} = 1.1\times10^4\ M^{-1}\ cm^{-1}$, depend on the concentrations of 8-oxodG as shown in Figure 3A.

The values of Y_{8oGR} grow rapidly with increasing concentrations of 8-oxodG to attain an apparent constant value of ~4.2 μM at [8-oxodG] = 60–80 μM (Figure 3A); in this range of 8-oxodG concentrations, the major fraction of AAPH-derived reactive species is trapped by 8-oxodG and a further increase in the 8-oxodG concentration does not increase Y_{8oGR}. After the initial 15–20 μs time interval, the formation of the 8-oxodG$^{\bullet+}$/8-oxodG(-H)$^{\bullet}$ radicals follows pseudo-first-order kinetics with the rate constant, k_a. The value of k_a does not depend on the concentration of 8-oxodG in the range of 10–100 μM (Figure 3B), indicating that the oxidation of 8-oxodG is rapid and the rate-determining step is the formation of the radical intermediates.

Additional mechanistic details concerning the formation of reactive species have been obtained from the laser flash photolysis of AAPH in the absence or presence of oxygen (26). These experiments have shown that the formation of the 2-amidinoprop-2-peroxyl radicals from AAPH-derived radicals (reaction 1) is completed within < 5 μs after the actinic laser flash and cannot be associated with the longer induction period of 10–15 μs observed in the case of the oxidation of 8-oxodG (inset in Figure 2). This is a clear indication that the ROO$^{\bullet}$ radicals do not react directly with 8-oxodG. The further transformation of these radicals to more reactive species is required for the one-electron oxidation of 8-oxodG to occur. We found that the activation of ROO$^{\bullet}$ radicals occurring during the induction period involves a cascade of chemical reactions (2–4) that are responsible for the formation of the secondary 2-amidinoprop-2-oxyl and the superoxide radicals (26):

$$\mathrm{AAPH} \xrightarrow[\mathrm{O_2}]{h\nu} 2\mathrm{ROO}^{\bullet} \quad (1)$$

$$\mathrm{ROO}^{\bullet} + \mathrm{ROO}^{\bullet} \rightarrow \mathrm{ROOOOR} \quad (2)$$

$$\mathrm{ROOOOR} \rightarrow x(2\mathrm{RO}^{\bullet} + \mathrm{O_2}) + \mathrm{products} \quad (3)$$

$$\mathrm{ROOOOR} \rightarrow y\mathrm{O_2}^{\bullet -} + \mathrm{products} \quad (4)$$

$$\mathrm{RO}^{\bullet} + 8-\mathrm{oxodG} \rightarrow \mathrm{ROH} + 8-\mathrm{oxodG(-H)}^{\bullet} \quad (5)$$

$$\mathrm{O_2}^{\bullet -} + \mathrm{C(NO_2)_4} \rightarrow \mathrm{O_2} + \mathrm{C(NO_2)_3}^{-} + {}^{\bullet}\mathrm{NO_2} \quad (6)$$

The rate-determining step of this process (reactions 2–4) is the recombination of RO$^{\bullet}$ radicals leading to the formation of tetraoxide, ROOOOR (reaction 2) and occurring with the rate constant, k_2 estimated as ~5×10^8 $M^{-1}s^{-1}$ (26). The decomposition of ROOOOR results in the formation of 2-amidinoprop-2-oxyl (reaction 3) and superoxide (reaction 4) radicals. The oxidation of 8-oxodG by RO$^{\bullet}$ radicals occurs via a step that is not rate-determining (reaction 5). From the values $k_a = 4.5\times10^4$ s^{-1} and [8-oxodG] = 80 μM, it follows that the lower limit for reaction 5 is $k_5 \approx 5\times10^8$ $M^{-1}s^{-1}$. Another secondary free radical arising from the bimolecular combination of ROO$^{\bullet}$ radicals (reaction 2) is the superoxide radical anion, $O_2^{\bullet -}$ (reaction 4) that was detected by the classical test reaction with tetranitromethane (reaction 6) (33). The characteristic absorption band of nitroform at 350 nm is clearly observed after laser pulse

excitation of AAPH in air-equilibrated buffer solutions containing tetranitromethane (26), which is consistent with reaction 6. Thus, the combination of $ROO^{\bullet}$ radicals generates a unique intermediate, the ROOOOR tetraoxide (34) that spontaneously decomposes to form $RO^{\bullet}$ and $O_2^{\bullet-}$ radicals (26), and these processes are responsible for the S-like shape of the kinetics of radical formation (inset, Figure 2).

The low activity of alkylperoxyl radicals with respect to direct oxidation of 8-oxodG, is supported by experiments with arachidonic and pentenoic acids (Figure 4)

ArAc is a typical polyunsaturated lipid molecule that plays an important role in inflammation-associated carcinogenesis (35,36). However, ArAc has a low solubility even in buffer mixtures containing 20% acetonitrile (30). To extend the concentration range, we used PcAc that is more soluble than ArAc. We found that the addition of both unsaturated acids suppresses the formation of $8\text{-oxodG}^{\bullet+}$/8-oxodG(-H)$^{\bullet}$ radicals (Figure 5).

The highly reactive $RO^{\bullet}$ radicals derived from the photolysis of AAPH add to the double bonds of these unsaturated acids to form β-alkoxyalkyl radicals (reaction 7), which in the presence of O_2, rapidly transforms to β-alkoxyperoxyl radicals (reaction 8) (30).

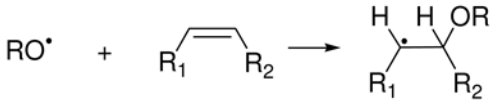

(7)

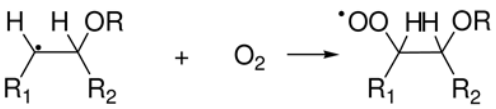

(8)

The latter radicals are less reactive than the parent $RO^{\bullet}$ radicals and do not react with 8-oxodG with observable rates. The β-alkoxyperoxyl radicals do not further transform to the β-alkoxyoxyl radicals as the 2-amidinoprop-2-peroxyl radicals do (reactions 2 and 3), and scavenging the 2-amidinoprop-2-oxyl radicals by unsaturated acids suppresses the oxidation of 8-oxodG.

End-Products of 8-Oxoguanine Oxidation Initiated by the Photolysis of AAPH

Laser flash photolysis experiments have shown that the photolysis of AAPH in the presence of oxygen generates oxidizing $RO^{\bullet}$ radicals, which mediate the fast one-electron oxidation of 8-oxodG (Figure 2), and reducing $O_2^{\bullet-}$ radicals (26) detected by the classical test reaction with tetranitromethane (33). According to our previous experiments, the 8-oxoG(-H)$^{\bullet}$ and $O_2^{\bullet-}$ radicals rapidly combine to form the 5-HOO-8-oxoG(-H) hydroperoxide that, in turn, rapidly decomposes to form dehydroguanidinohydantoin (32); the latter slowly transforms (within ~ 10 h at 37 °C) to the more stable oxaluric acid (37) (Figure 1). At the formal level, Gh_{ox} is the product of a four-electron oxidation of 8-oxoG and the $O_2^{\bullet-}$ ion radical acts as a three-electron oxidant in reactions with 8-oxoG(-H)$^{\bullet}$ radicals (32). Other products, the diastereomeric spiroiminodihydantoins (Sp), are the products of a two-electron oxidation of 8-oxoG (30,38). In our experiments, potential pathways of Sp formation might include the one-electron oxidation of 8-oxoG(-H)$^{\bullet}$ radicals by $ROO^{\bullet}/RO^{\bullet}$ radicals (30).

Here, we explore the nature of the end products produced by the oxidation of two substrates: (1) the 8-oxoG derivative 2′,3′,5′-tri-*O*-acetyl-8-oxo-7,8-dihydroguanosine, and (2) the 5′-d (CCATC[8-oxoG]CTACC) sequence used in our previous experiments (32). The acylated nucleoside products produced by the oxidation of tri-*O*-Ac-8-oxoG are more easily separated by reversed-phase HPLC. For instance, the diastereomeric spiroiminodihydantoin (Sp) nucleosides which, in the form of 2′-deoxynucleosides (dSp), typically elute in the void volume (39), can be easily detected in the acylated form (tri-*O*-Ac-Sp) together with other products (e.g., tri-*O*-Ac-Gh_{ox}, tri-*O*-Ac-Iz) using a regular reversed phase C18 column (30).

The photolysis of AAPH in air-equilibrated solutions containing tri-*O*-Ac-8-oxoG, leads to the disappearance of tri-*O*-Ac-8-oxoG as is evident from the decay of its absorption band at 295 nm (Figure 6).

The tri-*O*-Ac-8-oxoG oxidation products were isolated by reversed-phase HPLC and identified by LC-MS methods (Figure 7).

The well-separated fraction eluting at 29.4 min was identified as the dehydroguanidinohydantoin product, tri-*O*-Ac-Gh_{ox} detected at *m*/*z* 414.1 or M - 12, where M is the mass of the original tri-*O*-Ac-8-oxoG eluted at 31.3 min. The tri-*O*-Ac-Sp diastereomers (*m*/*z* 442.1 or M + 16), form in minor quantities and elute at 17.6 and 18.4 min. The retention times and masses of the molecular ions, $[M + H]^+$ of the products isolated from the irradiated samples were identical to those of the authentic standards (30).

Photolysis of AAPH in air-equilibrated buffer solutions also initiates the selective-oxidation of 8-oxoG in the single-stranded oligonucleotide, 5′-d(CCATC[8-oxoG]CTACC). The major oxidation product is the Gh_{ox} lesion as in the case of free nucleoside. The 5′-d(CCATC [Gh_{ox}]CTACC) adduct was isolated by reversed-phase HPLC (Figure 8A) and identified by MALDI-TOF/MS methods as described elsewhere (32, 37).

The time-dependent increase in the yields of the 5′-d(CCATC[Gh_{ox}]TACC) adducts is shown in the inset of Figure 8A. The addition of micromolar concentrations of Cu,Zn superoxide dismutase, Cu,Zn-SOD that induces the extremely fast catalytic dismutation of $O_2^{\bullet -}$ radicals to O_2 and H_2O_2 (40), suppresses the formation the Gh_{ox} products (Figure 7B). Here, we found that in the presence of Cu,Zn-SOD the yields of the Gh_{ox} lesions decrease by a factor of ~2 at Cu,Zn-SOD concentrations of 20 μM, and the further increase of the Cu,Zn-SOD concentration does not significantly reduce the yields. These observations indicate that the combination of $O_2^{\bullet -}$ and 8-oxodG$^{\bullet +}$/8-oxodG(-H)$^{\bullet}$ radicals is responsible for the formation of about one half of the Gh_{ox} lesions, and that the other half is associated with the combination of the ROO$^{\bullet}$ radicals with 8-oxodG$^{\bullet +}$/8-oxodG(-H)$^{\bullet}$ radicals. This mechanism can account for the somewhat lower yields of the Gh_{ox} lesions in the presence of Cu,Zn-SOD as reported earlier (30, 32).

Conclusion

The transient absorption measurements described here demonstrate that the laser photolysis of AAPH in oxygenated solutions initiates the efficient one-electron oxidation of 8-oxoG bases monitored by direct spectroscopic observations of the 8-oxodG$^{\bullet +}$/8-oxodG(-H)$^{\bullet}$ radicals. In principle, both alkylperoxyl radicals with E_7 = 1.0–1.1 V vs. NHE (41) and alkoxyl radicals with E_7 = 1.55–1.65 V vs NHE (42) are capable of induce electron abstraction from 8-oxoG with E_7 = 0.74 V vs. NHE (11). However, RO$^{\bullet}$ radicals are much more reactive than ROO$^{\bullet}$ radicals and directly oxidize 8-oxoG by a one-electron transfer mechanism to form the 8-oxodG$^{\bullet +}$/8-oxodG(-H)$^{\bullet}$ radicals. The detection of the 2-amidinoprop-2-oxyl radical spin adducts by ESR methods provides an alternative confirmation of the efficient formation of RO$^{\bullet}$ radicals from ROO$^{\bullet}$ radicals resulting from thermal (43,44) and photochemical (45) decomposition of AAPH in oxygenated aqueous solutions.

The combination of 8-oxoG$^{\bullet+}$/8-oxoG(-H)$^{\bullet}$ radicals with $O_2^{\bullet-}$/ROO$^{\bullet}$ radicals to form dehydroguanidinohydantoin lesions (Figure 1) is the major pathway for the formation of end products of 8-oxoG oxidation (30,32). In contrast, the one-electron oxidation of 8-oxoG$^{\bullet+}$/8-oxoG(-H)$^{\bullet}$ radicals by the ROO$^{\bullet}$ radicals to form the diastereometic Sp products (Figure 7), is less efficient than the radical combination pathway.

Acknowledgments

This work was supported by the National Institute of Environmental Health and Sciences (5 R01 ES 011589-08). The content is solely the responsibility of the authors and does not necessarily represent the official views of the National Institute of Environmental Health and Sciences or the National Institutes of Health. Components of this work were conducted in the Shared Instrumentation Facility at NYU that was constructed with support from a Research Facilities Improvement Grant (C06 RR-16572) from the National Center for Research Resources, National Institutes of Health. The acquisition of the ion trap mass spectrometer was supported by the National Science Foundation (CHE-0234863).

References

1. Anand P, Kunnumakkara AB, Sundaram C, Harikumar KB, Tharakan ST, Lai OS, Sung B, Aggarwal BB. Cancer is a preventable disease that requires major lifestyle changes. Pharm Res 2008;25:2097–2116. [PubMed: 18626751]
2. Beckman KB, Ames BN. Oxidative decay of DNA. J Biol Chem 1997;272:19633–19636. [PubMed: 9289489]
3. Grollman AP, Moriya M. Mutagenesis by 8-oxoguanine: An enemy within. Trends Genet 1993;9:246–249. [PubMed: 8379000]
4. Cole J, Skopek TR. International Commission for Protection Against Environmental Mutagens and Carcinogens. Working paper no. 3, Somatic mutant frequency, mutation rates and mutational spectra in the human population in vivo. Mutat Res 1994;304:33–105. [PubMed: 7506357]
5. Steenken S, Jovanovic SV. How easily oxidizable is DNA? One-electron reduction potentials of adenosine and guanosine radicals in aqueous solution. J Am Chem Soc 1997;119:617–618.
6. Henderson PT, Delaney JC, Gu F, Tannenbaum SR, Essigmann JM. Oxidation of 7,8-dihydro-8-oxoguanine affords lesions that are potent sources of replication errors in vivo. Biochemistry 2002;41:914–921. [PubMed: 11790114]
7. Henderson PT, Delaney JC, Muller JG, Neeley WL, Tannenbaum SR, Burrows CJ, Essigmann JM. The hydantoin lesions formed from oxidation of 7,8-dihydro-8-oxoguanine are potent sources of replication errors in vivo. Biochemistry 2003;42:9257–9262. [PubMed: 12899611]
8. Neeley WL, Essigmann JM. Mechanisms of formation, genotoxicity, and mutation of guanine oxidation products. Chem Res Toxicol 2006;19:491–505. [PubMed: 16608160]
9. Marnett LJ. Oxyradicals and DNA damage. Carcinogenesis 2000;21:361–370. [PubMed: 10688856]
10. Marnett LJ. Oxy radicals, lipid peroxidation and DNA damage. Toxicology 2002;181–182:219–222.
11. Steenken S, Jovanovic SV, Bietti M, Bernhard K. The trap depth (in DNA) of 8-oxo-7,8-dihydro-2′ deoxyguanosine as derived from electron-transfer equilibria in aqueous solution. J Am Chem Soc 2000;122:2373–2374.
12. Neta P, Grodkowski J, Ross AB. Rate constants for reactions of aliphatic carbon-centered radicals in aqueous solution. J Phys Chem Ref Data 1996;25:709–1050.
13. Barclay LRC, Locke SJ, MacNeil JM, VanKessel J, Burton GW, Ingold KU. Autoxidation of micelles and model membranes. Quantitative kinetic measurements can be made by using either water-soluble or lipid-soluble initiators with water-soluble or lipid-soluble chain-breaking antioxidants. J Am Chem Soc 1984;106:2479–2481.
14. Yamamoto Y, Haga S, Niki E, Kamiya E. Oxidation of lipids. V. Oxidation of methyl linoleate in aqueous dispersion. Bull Chem Soc Jpn 1984;57:1260–1264.
15. Gieseg SP, Pearson J, Firth CA. Protein hydroperoxides are a major product of low density lipoprotein oxidation during copper, peroxyl radical and macrophage-mediated oxidation. Free Radic Res 2003;37:983–991. [PubMed: 14670006]
16. Schnitzer E, Pinchuk I, Lichtenberg D. Peroxidation of liposomal lipids. Eur Biophys J 2007;36:499–515. [PubMed: 17380326]

17. Lucio M, Ferreira H, Lima JL, Reis S. Use of liposomes as membrane models to evaluate the contribution of drug-membrane interactions to antioxidant properties of etodolac. Redox Rep 2008;13:225–236. [PubMed: 18796242]
18. Yoshida Y, Itoh N, Saito Y, Hayakawa M, Niki E. Application of water-soluble radical initiator, 2,2′-azobis[2-(2-imidazolin-2-yl)propane] dihydrochloride, to a study of oxidative stress. Free Radic Res 2004;38:375–384. [PubMed: 15190934]
19. Cui Y, Kim DS, Park SH, Yoon JA, Kim SK, Kwon SB, Park KC. Involvement of ERK AND p38 MAP kinase in AAPH-induced COX-2 expression in HaCaT cells. Chem Phys Lipids 2004;129:43–52. [PubMed: 14998726]
20. Wada S, Tabuchi Y, Kondo T, Cui ZG, Zhao QL, Takasaki I, Salunga TL, Ogawa R, Arai T, Makino K, Furuta I. Gene expression in enhanced apoptosis of human lymphoma U937 cells treated with the combination of different free radical generators and hyperthermia. Free Radic Res 2007;41:73–81. [PubMed: 17164180]
21. Roche M, Tarnus E, Rondeau P, Bourdon E. Effects of nutritional antioxidants on AAPH- or AGEs-induced oxidative stress in human SW872 liposarcoma cells. Cell Biol Toxicol 2009;25:635–644. [PubMed: 19152116]
22. Paul T, Young MJ, Hill IE, Ingold KU. Strand cleavage of supercoiled DNA by water-soluble peroxyl radicals. The overlooked importance of peroxyl radical charge. Biochemistry 2000;39:4129–4135. [PubMed: 10747804]
23. Sanchez C, Shane RA, Paul T, Ingold KU. Oxidative damage to a supercoiled DNA by water soluble peroxyl radicals characterized with DNA repair enzymes. Chem Res Toxicol 2003;16:1118–1123. [PubMed: 12971799]
24. Ingold KU. Reactions of water-soluble alkylperoxyl radicals and superoxide with DNA, lipoproteins and phospholipid vesicles: the role played by electrostatic forces. Curr Med Chem 2003;10:2631–2642. [PubMed: 14529453]
25. Jung KJ, Lee EK, Yu BP, Chung HY. Significance of protein tyrosine kinase/protein tyrosine phosphatase balance in the regulation of NF-kappaB signaling in the inflammatory process and aging. Free Radic Biol Med 2009;47:983–991. [PubMed: 19596065]
26. Shao J, Geacintov NE, Shafirovich V. Oxidative modification of guanine bases initiated by oxyl radicals derived from photolysis of azo compounds. J Phys Chem B. 2010 submitted.
27. Niles JC, Wishnok JS, Tannenbaum SR. A novel nitration product formed during the reaction of peroxynitrite with 2′,3′,5′-tri-O-acetyl-7,8-dihydro-8-oxoguanosine: N-nitro-N′-[1-(2,3,5-tri-O-acetyl-beta-D-erythro-pentofuranosyl)- 2, 4-dioxoimidazolidin-5-ylidene]guanidine. Chem Res Toxicol 2000;13:390–396. [PubMed: 10813656]
28. Buettner GR, Jurkiewicz BA. Catalytic metals, ascorbate and free radicals: combinations to avoid. Radiat Res 1996;145:532–541. [PubMed: 8619018]
29. Shafirovich V, Dourandin A, Huang W, Luneva NP, Geacintov NE. Oxidation of guanine at a distance in oligonucleotides induced by two-photon photoionization of 2-aminopurine. J Phys Chem B 1999;103:10924–10933.
30. Crean C, Geacintov NE, Shafirovich V. Pathways of arachidonic acid peroxyl radical reactions and product formation with guanine radicals. Chem Res Toxicol 2008;21:358–373. [PubMed: 18159932]
31. Shafirovich V, Cadet J, Gasparutto D, Dourandin A, Huang W, Geacintov NE. Direct spectroscopic observation of 8-oxo-7,8-dihydro-2′-deoxyguanosine radicals in double-stranded DNA generated by one-electron oxidation at a distance by 2-aminopurine radicals. J Phys Chem B 2001;105:586–592.
32. Misiaszek R, Uvaydov Y, Crean C, Geacintov NE, Shafirovich V. Combination reactions of superoxide with 8-oxo-7,8-dihydroguanine radicals in DNA: Kinetics and end-products. J Biol Chem 2005;280:6293–6300. [PubMed: 15590679]
33. Rabani J, Mulac WA, Matheson MS. The pulse radiolysis of aqueous tetranitromethane. I. Rate constants and the extinction coefficient of eaq-. II. Oxygenated solutions. J Phys Chem 1965;69:53–70.
34. von Sonntag C, Schuchmann HP. The elucidation of peroxyl radical reactions in aqueous solution with the help of radiation-chemical methods. Angew Chem, Int Ed Engl 1991;30:1229–1253.

35. Chen X, Sood S, Yang CS, Li N, Sun Z. Five-lipoxygenase pathway of arachidonic acid metabolism in carcino-genesis and cancer chemoprevention. Curr Cancer Drug Targets 2006;6:613–622. [PubMed: 17100567]
36. Nakanishi M, Rosenberg DW. Roles of cPLA2alpha and arachidonic acid in cancer. Biochim Biophys Acta 2006;1761:1335–1343. [PubMed: 17052951]
37. Duarte V, Gasparutto D, Yamaguchi LF, Ravanat JL, Martinez GR, Medeiros MHG, Di Mascio P, Cadet J. Oxaluric acid as the major product of singlet oxygen-mediated oxidation of 8-oxo-7,8-dihydroguanine in DNA. J Am Chem Soc 2000;122:12622–12628.
38. Luo W, Muller JG, Rachlin EM, Burrows CJ. Characterization of spiroiminodihydantoin as a product of one-electron oxidation of 8-oxo-7,8-dihydroguanosine. Org Lett 2000;2:613–616. [PubMed: 10814391]
39. Ravanat JL, Cadet J. Reaction of singlet oxygen with 2′-deoxyguanosine and DNA. Isolation and characterization of the main oxidation products. Chem Res Toxicol 1995;8:379–388. [PubMed: 7578924]
40. Fridovich I. Superoxide radical and superoxide dismutases. Annu Rev Biochem 1995;64:97–112. [PubMed: 7574505]
41. Jovanovic SV, Jankovic I, Josimovic L. Electron-transfer reactions of alkylperoxy radicals. J Am Chem Soc 1992;114:9018–9021.
42. Koppenol WH. Oxyradical reactions: from bond-dissociation energies to reduction potentials. FEBS Lett 1990;264:165–167. [PubMed: 2358063]
43. Krainev AG, Bigelow DJ. Comparison of 2,2′-azobis(2-amidinopropane) hydrochloride (AAPH) and 2,2′-azobis(2,4-dimethylvaleronitrile) (AMVN) as free radical initiators: a spin-trapping study. J Chem Soc Perkin Trans 1996;2:747–754.
44. Wahl RUR, Zeng L, Madison SA, DePinto RL, Shay BJ. Mechanistic studies on the decomposition of water soluble azo-radical-initiators. J Chem Soc Perkin Trans 1998;2:2009–2017.
45. Kohri S, Fujii H, Oowada S, Endoh N, Sueishi Y, Kusakabe M, Shimmei M, Kotake Y. An oxygen radical absorbance capacity-like assay that directly quantifies the antioxidant's scavenging capacity against AAPH-derived free radicals. Anal Biochem 2009;386:167–171. [PubMed: 19150323]

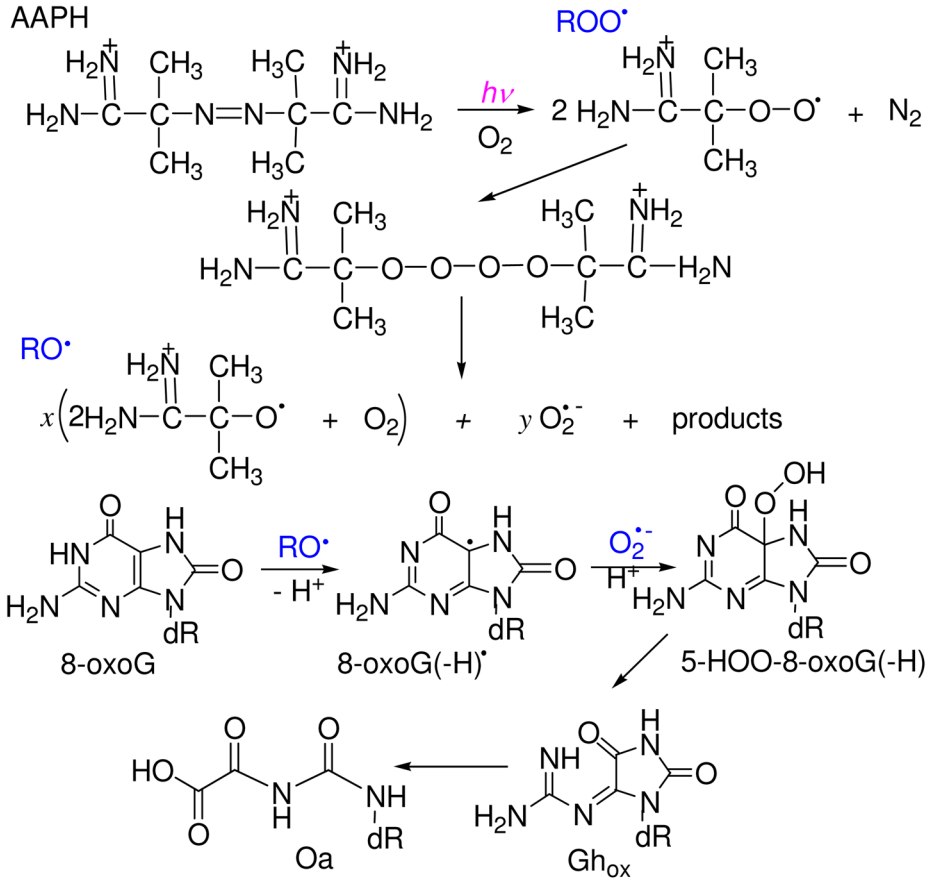

Figure 1.

Oxidation of 8-oxoguanine initiated by the photolysis of AAPH in oxygenated solutions. Peroxyl radicals, $ROO^{\bullet}$ produced by the photolysis of AAPH recombine to form the tetraoxide ROOOOR. The spontaneous cleavage of ROOOOR generates highly reactive oxyl radicals ($RO^{\bullet}$) and superoxide radicals ($O_2^{\bullet -}$) with yields of *x* and *y*, respectively.

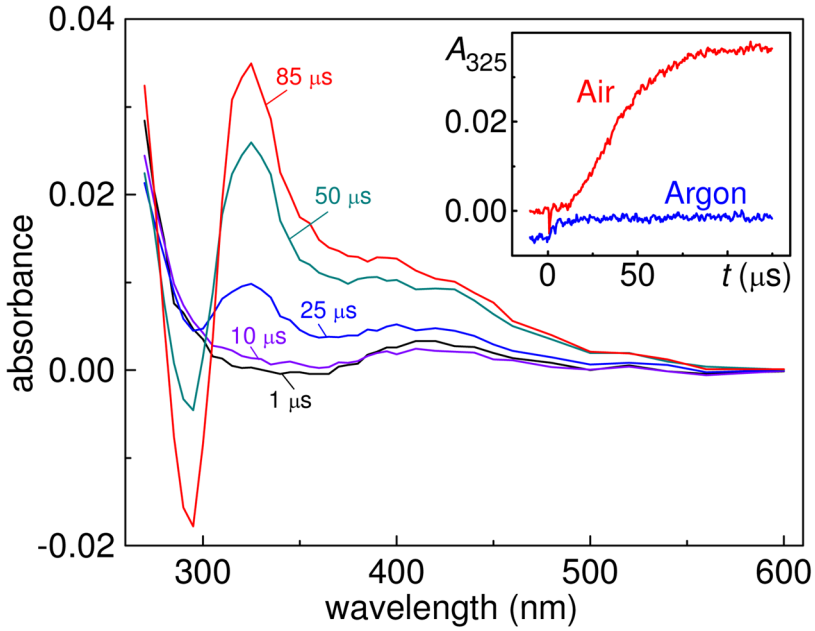

Figure 2.

One-electron oxidation of 8-oxodG induced by laser flash photolysis of AAPH in air-equilibrated buffer solutions (pH 7, $[O_2]$ = 0.27 mM). Transient absorption spectra were recorded at the indicated delay times after a 355 nm single laser pulse excitation (E = 20 mJ/pulse/cm^2) of 20 mM AAPH and 0.03 mM 8-oxodG. The inset shows the kinetic profile of 8-oxodG$^{\bullet+}$/8-oxodG(-H)$^{\bullet}$ radicals at 325 nm in air-equilibrated (red trace) and argon-purged (blue) solutions.

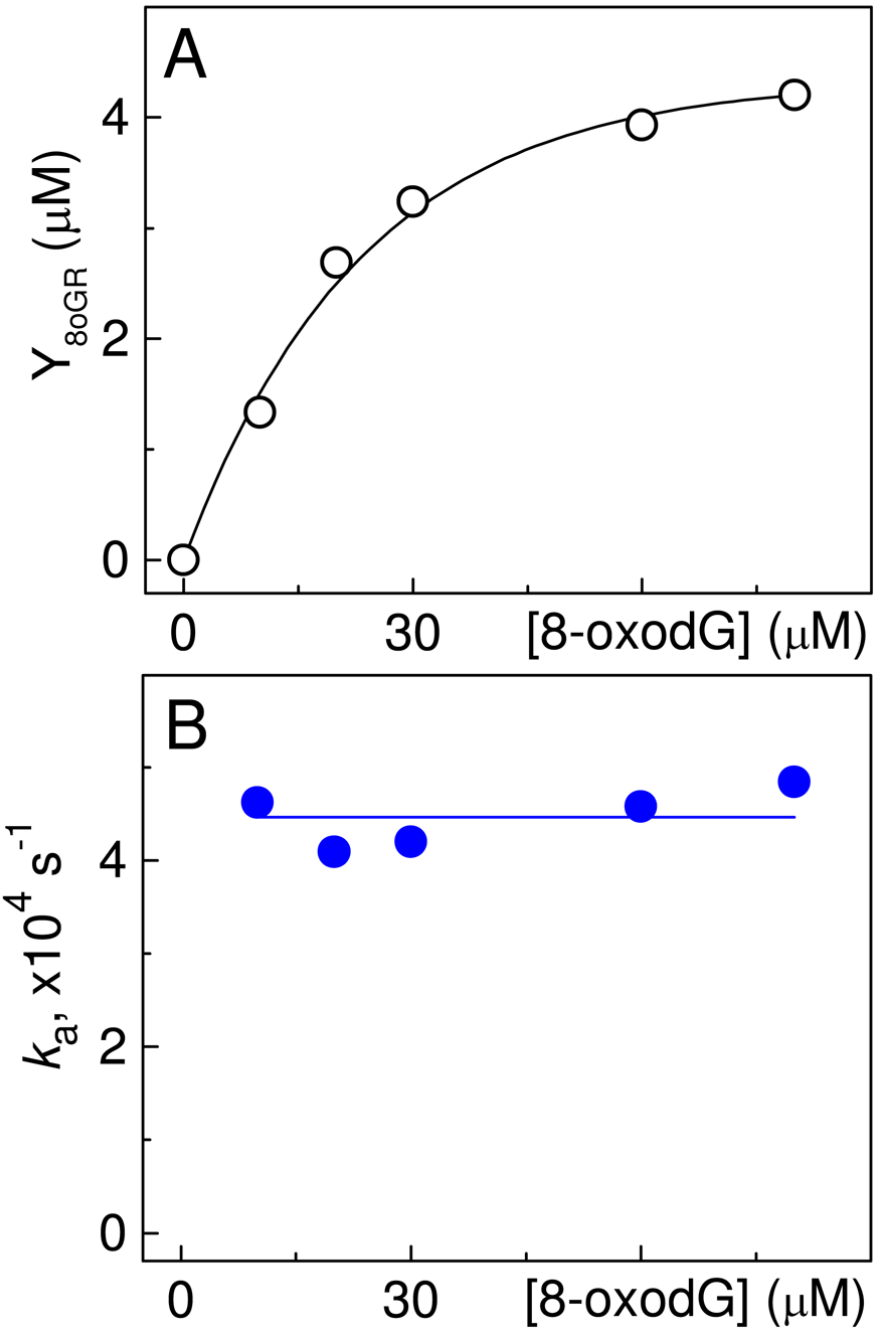

Figure 3.
Effect of 8-oxodG concentration on the yields (Y_{8oGR}) and rate constants (k_a) of 8-oxodG$^{\bullet+}$/ 8- oxodG(-H)$^{\bullet}$ formation. [AAPH] = 20 mM; E = 20 mJ/pulse/cm^2.

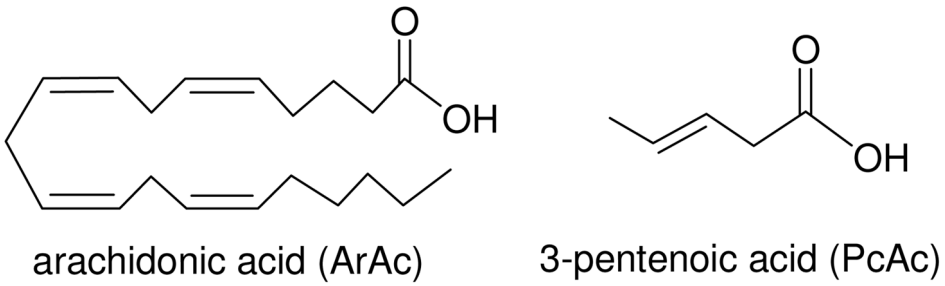

arachidonic acid (ArAc) 3-pentenoic acid (PcAc)

Figure 4.
Structures of unsaturated fatty acids.

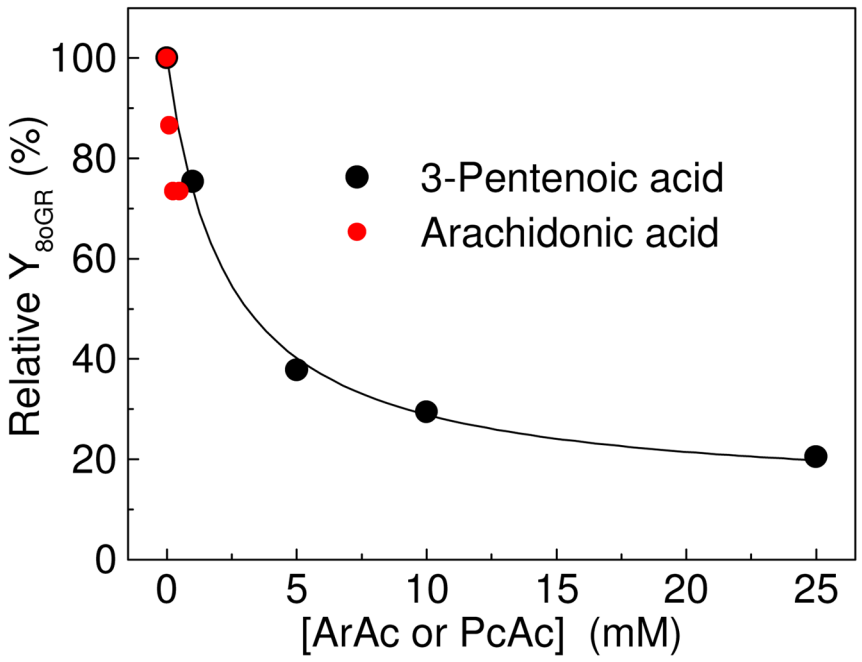

Figure 5.
Effect of ArAc or PcAc concentrations on the relative yields of 8-oxodG$^{\bullet+}$/8-oxodG(-H)$^{\bullet}$ radicals. The experiments with ArAc were performed in buffer solutions containing 20% acetonitrile. [AAPH] = 20 mM; [8-oxodG] = 20 μM, E = 20 mJ/pulse/cm^2.

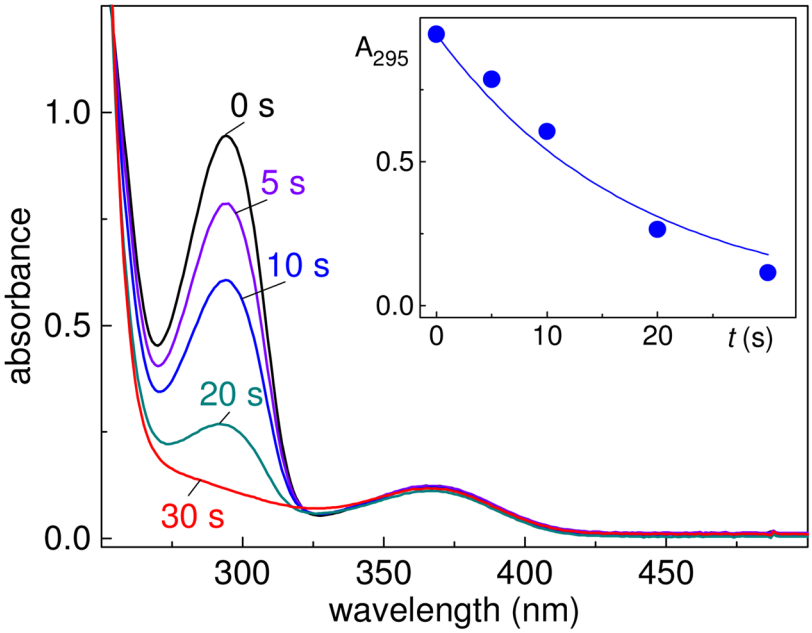

Figure 6.

Oxidation of tri-*O*-Ac-8-oxoG (λ_{max} = 295 nm) initiated by the photolysis of AAPH (λ_{max} = 365 nm) in air-equilibrated phosphate buffer solutions. The solutions were photolyzed using 340–390 nm steady-state irradiation (~100 mW/cm^2) from a 100 W Xe arc lamp for fixed periods of time. The inset shows the decay of tri-*O*-Ac-8-oxoG (100 μM) absorbance as a function of time during the course of AAPH (300 μM) photolysis.

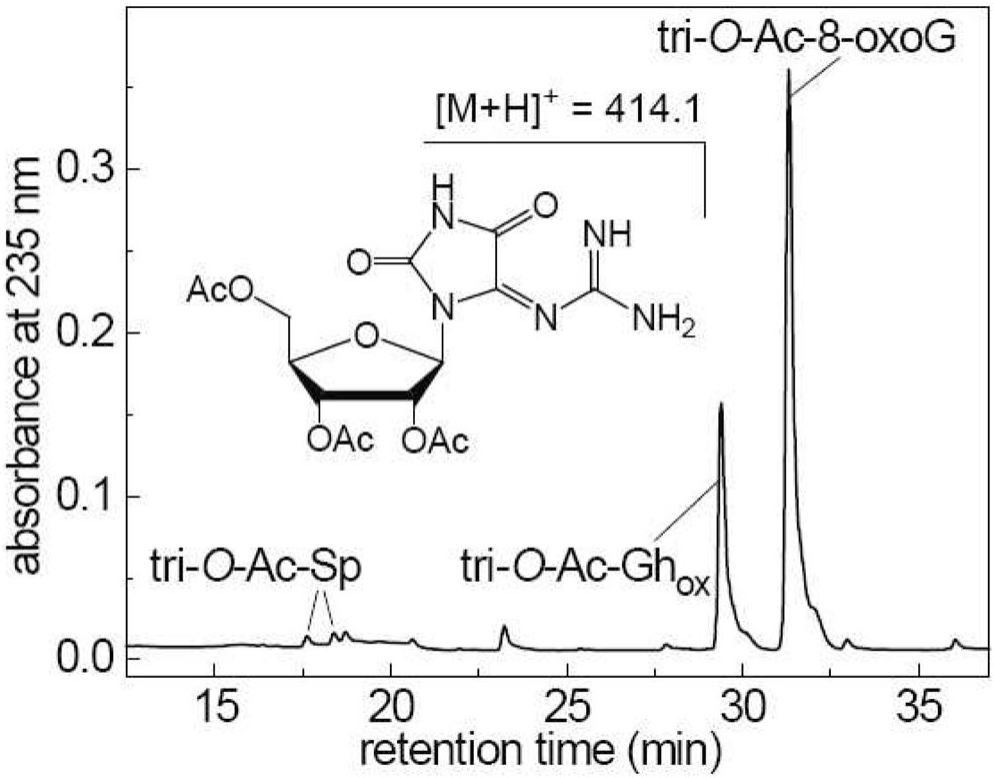

Figure 7.

End products derived from the oxidation of tri-*O*-Ac-8-oxoG (100 μM) initiated by the photolysis of AAPH (300 μM) in air-equilibrated phosphate buffer solutions. The solutions were photolyzed using 340–390 nm steady-state irradiation (~100 mW/cm^2) from a 100 W Xe arc lamp for fixed periods of time. Reversed-phase HPLC elution profile of the sample irradiated for 10 s. HPLC elution conditions (detection of products at 235 nm): 5–40% gradient of acetonitrile in 20 mM ammonium acetate over 60 min at flow rate of 1 mL/min. The tri-*O*-Ac-Gh$_{ox}$ elutes at 29.4 min, and the unmodified tri-*O*-Ac-8-oxoG at 31.3 min. The tri-*O*-Ac-Sp diastereomers are formed in minor quantities and elute at 17.6 and 18.4 min.

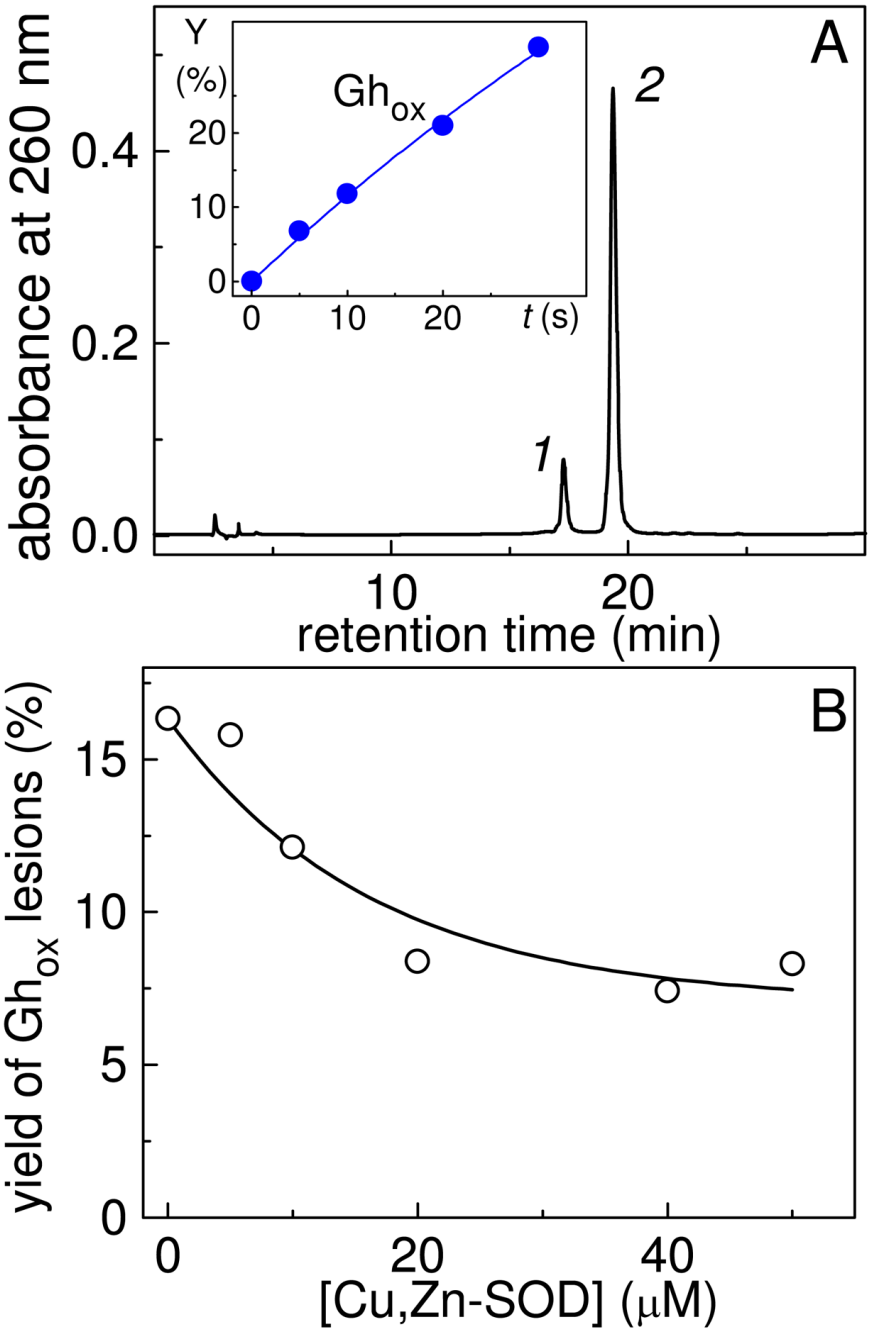

Figure 8.

End-products derived from the oxidation of 5′-d(CCATC[8-oxoG]TACC) (10 μM) initiated by photolysis of AAPH (300 μM) in air-equilibrated phosphate buffer solutions. The solutions were photolyzed using 340–390 nm steady-state irradiation (~100 mW/cm^2) from a 100 W Xe arc lamp for fixed periods of time. (A) Reversed-phase HPLC elution profile of a sample irradiated for 10 s. HPLC elution conditions (detection of products at 260 nm): 5–20% gradient of acetonitrile in 50 mM triethylammonium acetate (pH 7) over 60 min at flow rate of 1 mL/min. The 5′-d(CCATC[Gh$_{ox}$]TACC) adduct ***2*** elutes at 17.3 min, and the unmodified 5′-d(CCATC[8-oxoG]TACC) sequence ***1*** at 19.3 min. The inset show the time-dependent yields

of the 5′-d(CCATC[Gh_{ox}]TACC) adducts. (B) Effect of Cu,Zn-SOD on the yields of 5′-d (CCATC[Gh_{ox}]TACC) adducts.